Effects of Chain Ends and Three-Segment Interactions on Second and Third Virial Coefficients of Four-Arm Star Polystyrenes

By Yasuhiro NISHI,[1] Yo NAKAMURA,[2,*] and Takashi NORISUYE[1]

Second and third virial coefficients (A_2 and A_3, respectively) for cyclohexane solutions (34.5 °C) of three four-arm star polystyrene (PS) samples with a benzyl group at each arm end (4SPS-Bz) and two four-arm star PS samples with a *sec*-butyl group at each arm end (4SPS-Bu) were determined as functions of weight-average molecular weight M_w lower than 1.5×10^4. As in the case for linear PS with benzyl ends, A_2 for 4SPS-Bz at the theta temperature (34.5 °C), where A_2 vanishes for sufficiently high M_w, was negative and decreased with lowering M_w in contrast to the increase of positive A_2 for 4SPS-Bu. The negative A_2 for 4SPS-Bz was ascribed to the effects of three-segment interactions and binary interactions between middle and junction point segments, while the positive A_2 for 4SPS-Bu was explained as due to the effects from arm ends. These findings reveal that the previously observed lowering in apparent theta temperature (with decreasing M_w), where $A_2 = 0$ for a given M_w, for four-arm star polystyrene is attributed to the arm-end effect. The values of A_3 for both 4SPS-Bz and 4SPS-Bu were positive and increased with decreasing M_w at the theta temperature, showing significant three-segment interactions among two middle and one junction point or one arm-end segment.
KEY WORDS: Virial Coefficient / Light Scattering / Star Polymer / Chain-End Effect / Ternary-Cluster Integral / Theta Temperature /

Recently, Mizuno *et al.*[1] found from light scattering measurements that the second virial coefficient A_2 of linear polystyrene (PS) with benzyl ends (benzyl-PS) in cyclohexane at the theta point Θ (34.5 °C) becomes negative and decreases with decreasing weight-average molecular weight M_w in contrast to positive and increasing A_2 for linear PS with a butyl group at one of the chain ends (butyl-PS),[2,3] where Θ is defined as the temperature at which A_2 vanishes for sufficiently high molecular weight M. They explained the negative A_2 for benzyl-PS as due to the effects from three-segment interactions with negligibly small chain-end effects. On the other hand, for butyl-PS the end effects[4] on A_2 were predominant, demonstrating that the chain-end groups strongly affect A_2 of low M polystyrene ($M_w < 3 \times 10^4$) at Θ.

It is well-known for star polymers that the apparent theta temperature Θ_{app}, where $A_2 = 0$ for a given M, decreases with lowering M.[5–11] This is equivalent to an increase in A_2 with decreasing M at a fixed temperature Θ. Such molecular weight dependence of Θ_{app} (or opposite dependence of A_2 at Θ) for star polymers has been interpreted as due to effects of three-segment interactions by theories based on the smoothed-density model.[12,13] However, a more rigorous perturbation calculation[14] predicts a decrease in A_2 at Θ with decreasing M for f (the number of arms) less than five.[15] This prediction, contradictory to the behavior of experimental A_2 for star polymers, at least, with $f \leq 4$, prompted us to examine the end effects on A_2 of four-arm star PS as was done for linear PS. We note that the previously investigated star polystyrene samples, anionically synthesized with butyllithium,[16–20] had a butyl

group at each arm end.

In the present work, we prepared three and two low molar mass samples of four-arm star polystyrenes with a benzyl group (4SPS-Bz) and a butyl group (4SPS-Bu) at each arm end, respectively, and determined their A_2 and A_3 (the third virial coefficient) in cyclohexane at Θ by light scattering. Our interest in A_3 was to see whether the third coefficients for the two star polymers increase with lowering M_w as was found for linear polystyrenes by Mizuno *et al.*[1] The results are analyzed below in comparison with published A_2 and A_3 data for liner PS in the same solvent to estimate the binary and ternary segment interactions associated with end groups, *i.e.*, the segments at the junction point and the arm ends.

EXPERIMENTAL

Samples

All polymer samples were anionically polymerized under nitrogen atmosphere. Samples of 4SPS-Bz were prepared by the coupling reaction[9,15] of 1,2-bis(trichlorosilyl)ethane and living polystyrene polymerized with benzyllithium. Although the coupling reagent has six reactive sites in each molecule, only four polystyryl anions can react directly with one coupling reagent molecule to yield four-arm star polystyrene;[9] we note that two unreacted coupling sites (Si–Cl bonds) involved in the junction point segment may generate hydroxyl groups upon exposure to air. Samples of 4SPS-Bu were synthesized by the coupling reaction of the same reagent with polystyryl anions prepared from *sec*-butyllithium. The crude samples were

[1]Department of Macromolecular Science, Osaka University, 1-1 Machikaneyama-cho, Toyonaka 560-0043, Japan
[2]Department of Polymer Chemistry, Kyoto University, Katsura, Kyoto 615-8510, Japan
*To whom correspondence should be addressed (E-mail: yonaka@molsci.polym.kyoto-u.ac.jp).

Table I. Results from light scattering, SEC, and viscometry for benzyl- and butyl-end four arm star polystyrenes in cyclohexane at 34.5 °C

Sample	M_w	f	$(M_w/M_n)^a$	$[\eta]/$ cm^3 g^{-1}	$10^4 A_2/$ cm^3 mol g^{-2}	$10^3 A_3/$ cm^6 mol g^{-3}
4S0.9-Bu	3,570	3.6	1.08	4.0_0	3.7	1.1
4S2.2-Bu	8,870	4.0	1.09	5.4_9	2.1	0.7_5
4S0.8-Bz	3,030	3.8	1.11	3.9_0	−2.9	2.0
4S2.0-Bz	7,970	4.0	1.07	6.2_9	−1.1	0.9_2
4S4.0-Bz	14,500	3.7	1.06	8.3_2	$−0.7_5$	1.0

^{a}for precursor

purified by successive fractional precipitation with cyclohexane as the solvent and methanol as the precipitant. Complete removal of the linear precursor polymers contained was confirmed by the size-exclusion chromatography (SEC). In this way, we obtained three 4SPS-Bz (4S0.8-Bz, 4S2.0-Bz, and 4S4.0-Bz) and two 4SPS-Bu (4S0.9-Bu and 4S2.2-Bu) samples.

Table I summarizes the values of M_w determined by light scattering for all the star polymer samples (see RESULTS for the procedure), the weight to number-average molecular weight ratios (M_w/M_n) for the linear precursors determined by SEC, and the molecular weight ratios f ($= M_w$ of the star sample/ that of the linear precursor); the M_w values of the linear precursors for 4S0.8-Bz, 4S4.0-Bz, and 4S2.2-Bu were determined by light scattering and those for the rests (4S0.9-Bu and 4S2.0-Bz) were by MALDI-TOF mass spectroscopy because of the paucity of the sample. The f values smaller than 4 do not necessarily mean that the samples contain star molecules with smaller arm numbers, because their molecular weights are affected by fractionation. Intrinsic viscosities $[\eta]$ in cyclohexane at 34.5 °C measured by use of a conventional Ubbelohde type capillary viscometer are also summarized in the fifth column of the table. Except for 4S2.2-Bu, they are in substantial agreement with the values calculated from the measured M_w and the known relation[15]

$$[\eta]/\text{cm}^3\,\text{g}^{-1} = 6.6 \times 10^{-2} M_w^{0.5}$$

for 4SPS-Bu with $M_w \geq 8.5 \times 10^4$; for 4S2.2-Bu, $[\eta]$ is about 12% smaller than the calculated value.

Preparation of Solutions

Cyclohexane was refluxed over sodium for 5 h and then fractionally distilled. The polymer mass concentration c was calculated from the gravimetrically determined polymer weight fraction w according to the relation

$$c = w\rho_0/[1 - w + \bar{v}\rho_0 w]$$

Here, ρ_0 and $\bar{v}$ denote the solvent density and the partial specific volume of the solute, respectively. The latter value in cyclohexane at 34.5 °C was determined by use of an Anton-Paar densitometer to be 0.945, 0.939, 0.927, 0.930, and 0.934 cm^3 g^{-1} for 4S0.9-Bu, 4S2.2-Bu, 4S0.8-Bz, 4S2.0-Bz, and 4S4.0-Bz, respectively. While $\bar{v}$ for 4SPS-Bu is smaller for the higher M_w, that for 4SPS-Bz is an increasing function of M_w.

Light Scattering

Scattering intensities were measured in cyclohexane at 34.5 °C on a Fica-50 light scattering photometer in an angular range from 30 to 150°. Vertically polarized incident light of 436-nm wavelength was used. The apparatus was calibrated with benzene at 25 °C with the Rayleigh ratio for the unpolarized light at 90° taken as 46.5×10^{-6} cm^{-1}.[21] Test solutions were optically clarified by filtration through Millipore filters with 0.45-μm pore size.

The excess reduced intensity R_θ of unpolarized scattered light at the scattering angle θ was obtained for vertically polarized incident light by subtracting the reduced intensity for the pure solvent from that for the solution. Optical anisotropy correction was made according to the conventional method with the depolarization ratio ρ_u determined for both solution and solvent (see ref 22). The data of Kc/R_θ obtained were extrapolated to zero angle using the $(Kc/R_\theta)^{1/2}$ vs $\sin^2(\theta/2)$ plot,[23] where K denotes the optical constant.

The specific refractive index increment $\partial n/\partial c$ at 436 nm was determined to be 0.183, 0.178, 0.187, 0.184, and 0.182 cm^3 g^{-1} for 4S0.9-Bu, 4S2.2-Bu, 4S0.8-Bz, 4S2.0-Bz, and 4S4.0-Bz, respectively, in cyclohexane at 34.5 °C using a modified Schulz-Cantow type differential refractometer.

RESULTS

Figure 1 illustrates the concentration dependence of Kc/R_0 (the zero-angle value of Kc/R_θ) for star polystyrenes in cyclohexane at 34.5 °C. The curves for the butyl-end star samples monotonically rise with c, while those for the benzyl-end star samples once decline and then rise with c.

These Kc/R_0 data were analyzed in terms of the Bawn plot[24] of $S(c_1, c_2)$ against $(c_1 + c_2)$, where $S(c_1, c_2)$ is defined by[25]

$$S(c_1, c_2) \equiv \frac{(Kc/R_0)_{c=c_2} - (Kc/R_0)_{c=c_1}}{c_2 - c_1}$$
$$= 2A_2 + 3A_3(c_1 + c_2) + \dots \quad (1)$$

with $(Kc/R_0)_{c=c_i}$ denoting (Kc/R_0) at $c = c_i$ ($i = 1, 2$). Figure 2 shows the Bawn plots for four-arm star polystyrene samples in cyclohexane at 34.5 °C, where pairs of data for neighboring c_1 and c_2 in a series of polymer concentrations are omitted since they were less accurate. The intercept and slope of each line give A_2 and A_3, respectively, which are summarized in Table I. Weight-average molecular weights were determined by extrapolating M_{app} [$\equiv (Kc/R_0 - 2A_2c - 3A_3c^2)^{-1}$] to $c = 0$ according to the equation.

$$Kc/R_0 = 1/M_w + 2A_2c + 3A_3c^2 \quad (2)$$

The curves in Figure 1 actually representing this equation with M_w, A_2, and A_3 in Table I closely fit the data points.

The molecular weight dependence of A_2 for the two four-arm star polymers is shown in Figure 3, in which A_2 for 4SPS-Bu (the filled squares and diamonds[15]) is positive and increases with decreasing M_w, while that for 4SPS-Bz (the unfilled squares) is negative and decreases with decreasing M_w. This sharp contrast can also be seen for A_2 of linear polystyrenes
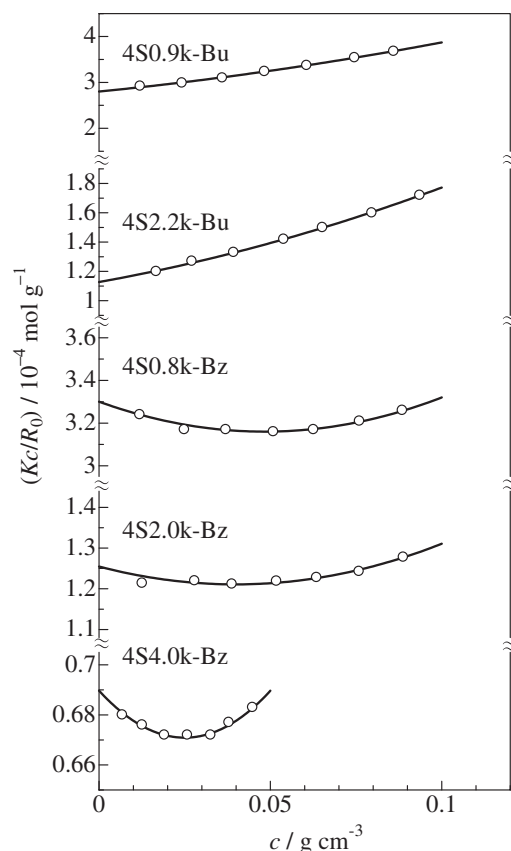
Figure 1. Plots of Kc/R_0 against c for four-arm star polystyrene samples in cyclohexane at 34.5 °C.

Figure 2. Bawn plots for four-arm star polystyrene samples in cyclohexane at 34.5 °C.

with butyl (the half-filled circles[3]) and benzyl (the unfilled circles[1]) ends in the figure. When compared at the same M_w, the absolute values of A_2 are larger for the star polymers than those for the linear polymers with the corresponding end groups.

Figure 4 shows that A_3's for both 4SPS-Bz (the unfilled squares) and 4SPS-Bu (the filled squares and diamonds[15]) are positive and increase with decreasing M_w and that the former is systematically larger than the latter. It can be seen in the figure that linear polystyrenes with benzyl (the unfilled circles) and butyl (the half-filled circles) ends exhibit the same tendency.

DISCUSSION

Second Virial Coefficient

The second virial coefficient for an f-arm star polymer with a not-too high M at Θ may be expressed as a sum of the contribution $A_2{}^0$ from residual ternary interactions[15] and that $A_2{}^{(E)}$ from chain ends[4] by

$$A_2 = A_2{}^0 + A_2{}^{(E)} \tag{3}$$

$$A_2{}^0 = \frac{N_A n^2}{2M^2}\left\{ \frac{4\sqrt{f}}{\sqrt{n}}[(f-1)(2-\sqrt{2})-2]\left(\frac{3}{2\pi b^2}\right)^{3/2}\beta_3 \right\} \tag{4}$$
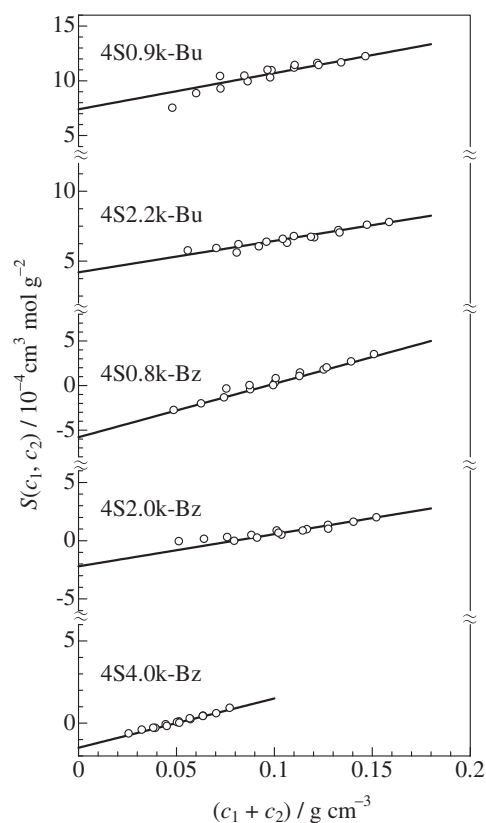
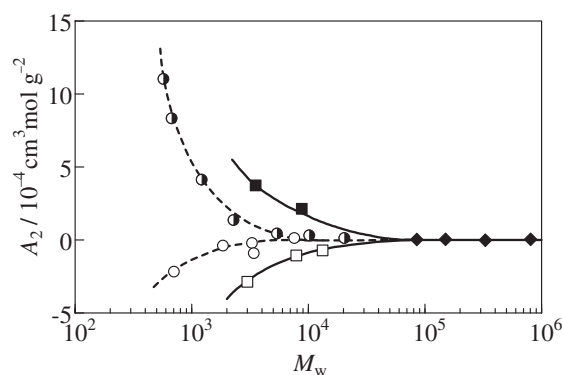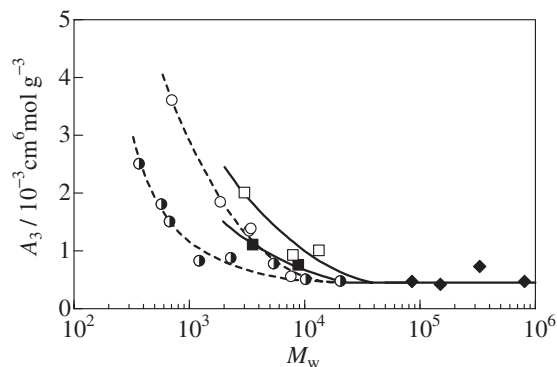$$A_2{}^{(E)} = a_1 M^{-1} + O(M^{-2}) \tag{5}$$

Figure 3. Molecular weight dependence of second virial coefficient for 4SPS-Bz (unfilled squares), 4SPS-Bu (filled squares and diamonds[15]), benzyl-PS (unfilled circles),[1] and butyl-PS (half-filled circles)[3] in cyclohexane at 34.5 °C. Lines are eye guides.

Here, N_A is the Avogadro constant, n is the total segment number, b is the effective bond length, β_3 is the ternary-cluster integral for the interaction among three middle segments, and a_1 is the coefficient for the contribution from binary interactions between middle and arm-end (or junction point) segments, given by

$$a_1 = \frac{N_A}{M_0}(f\beta_{01} + \beta_{02}) \tag{6}$$

in which M_0 is the molecular weight of the repeating unit and

Figure 4. Molecular weight dependence of third virial coefficient for 4SPS-Bz (unfilled squares), 4SPS-Bu (filled squares and diamonds[15]), benzyl-PS (unfilled circles),[1] and butyl-PS (half-filled circles)[3] in cyclohexane at 34.5 °C. Lines are eye guides.
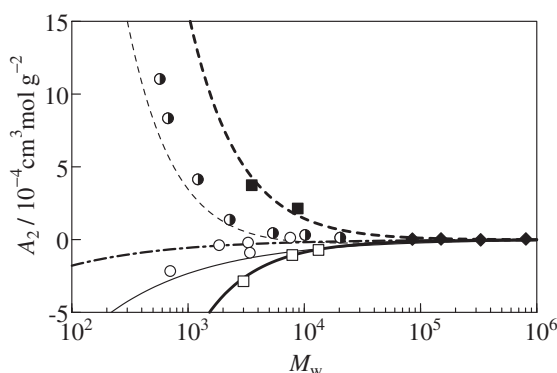
Figure 5. Comparison between measured and calculated second virial coefficients for 4SPS-Bz, 4SPS-Bu, benzyl-PS, and butyl-PS in cyclohexane at 34.5 °C. The symbols are the same as those in Figure 3. The lines represent theoretical values (see the text for the details).

β_{ij} is the excess binary-cluster integral[4] for the interaction between segments i and j, with the subscripts 0, 1, and 2 denoting the middle, arm end, and junction point segments, respectively; note that the binary-cluster integral for the segment pair i and j is equal to $\beta_{ij} + \beta_{00}$. Eq 4, the first-order perturbation result, predicts negative A_2 for $f \leq 4.41$ if the end effect is negligibly small.

The dot-dashed line in Figure 5 represents the values of A_2^0 calculated from eq 4 for four-arm star polystyrene with $b = 0.74$ nm (from the unperturbed gyration radius for high molecular weight PS in cyclohexane[26] at Θ) and $\beta_3 = 4 \times 10^{-3}$ nm^6 (from A_3 data[27] for high M_w at Θ). This perturbation equation predicts the negative A_2, being consistent with the data for 4SPS-Bz (the unfilled squares). However, the line is far above the data points for this star polymer, indicating that possible end effects must contribute to lowering A_2.

It was previously found that $A_2^{(E)}$ for benzyl-PS is negligibly small.[1] This is demonstrated by the fact that in Figure 5, the thin solid line, which represents A_2^0 calculated from eq 4 for $f = 1$ with $\beta_3 = 4 \times 10^{-3}$ nm^6, comes close to the data points (the unfilled circles) for benzyl-PS.[1] We note that a closer fit can be obtained if the chain stiffness is

considered.[28] Because the chemical structure of both chain ends of benzyl-PS is the same as that of the arm end of 4SPS-Bz, β_{01} for the binary interaction between middle and arm-end segments of 4SPS-Bz should be negligible, and the leading term of $A_2^{(E)}$ (eq 5) may be written as

$$A_2^{(E)} = \frac{N_A}{M_0 M} \beta_{02} \quad \text{(for 4SPS-Bz)} \tag{7}$$

The thick solid line in Figure 5 shows the theoretical A_2 obtained by adding this $A_2^{(E)}$ (eq 7 with $\beta_{02} = -0.12$ nm^3) to eq 4 (the dot-dashed line). Its fit to the unfilled squares allows us to conclude that the decrease in A_2 with lowering M_w for 4SPS-Bz is due to the combination effect of the ternary-cluster interaction and the binary interaction between middle and junction point segments, though the attractive binary interaction indicated by the negative β_{02} is not self-explanatory.

For butyl-end star polystyrene 4SPS-Bu, $A_2^{(E)}$ may be written

$$A_2^{(E)} = \frac{N_A}{M_0 M} (4\beta'_{01} + \beta_{02}) \quad \text{(for 4SPS-Bu)} \tag{8}$$

Here, β'_{01} represents the excess binary-cluster integral for a pair of middle and butyl-end segments. Because the chemical structure of the junction point of 4SPS-Bu is the same as that of 4SPS-Bz, β_{02} for 4SPS-Bu may be set equal to that for 4SPS-Bz. The thick dashed line in Figure 5 indicates the A_2 values calculated from eqs 3, 4, and 8 with β'_{01} taken to be 0.10 nm^3 so as to give a close fit to the filled squares and diamonds. Eq 4 for A_2^0 with $f = 1$ and $\beta_3 = 4 \times 10^{-3}$ nm^6 and the relation $A_2^{(E)} = N_A \beta'_{01}/(M_0 M)$ with $\beta'_{01} = 0.10$ nm^3 give A_2 of butyl-PS the thin dashed line which comes close to the data points (the half-filled circles) for the linear polymer. This β'_{01} estimated for 4SPS-Bu is considerably larger than the value 0.032 nm^3 obtained for butyl-PS by Einaga *et al.*,[3] who considered both M^{-1} and M^{-2} terms in eq 5. However, the difference is immaterial because these authors did not take into account A_2^0. In conclusion, the increase in A_2 (equivalent to the decrease in Θ_{app}) with lowering M_w for 4SPS-Bu is due to the effect not of three-segment interactions but of the butyl arm end whose contribution to A_2 surpasses the negative contributions of three-segment interactions and binary interactions between middle and junction point segments.

Third Virial Coefficient

The third virial coefficient for f-arm star chains at Θ may be expressed as a sum of the ternary-cluster term[29] A_3^0 and the chain-end contribution[30] $A_3^{(E)}$ by
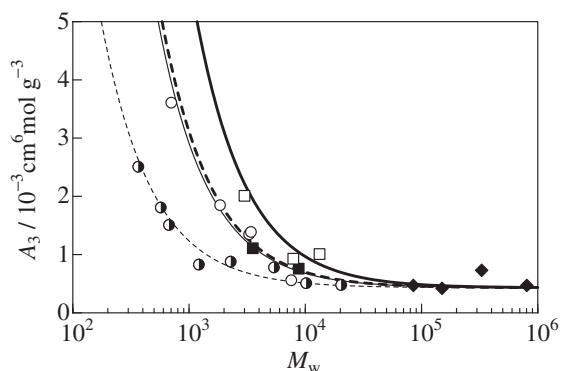
$$A_3 = A_3^0 + A_3^{(E)} \tag{9}$$

where

$$A_3^0 = \frac{N_A^2 n^3}{3M^3} \beta_3 \tag{10}$$

$$A_3^{(E)} = \frac{N_A^2 n^2}{M^3} (f + 1)\beta_{3,1} \tag{11}$$

when the end effect is considered up to the order of M^{-1} (or

Figure 6. Comparison between measured and calculated third virial coefficients for 4SPS-Bz, 4SPS-Bu, benzyl-PS, and butyl-PS in cyclohexane at 34.5 °C. The symbols are the same as those in Figure 4. The lines represent the theoretical values calculated from eq 9 with eqs 10 and 11 (see the text for the parameters used).

n^{-1}). In eq 11, $\beta_{3,1}$ is the mean ternary-cluster integral defined by $(f+1)\beta_{3,1} = f\beta_{001} + \beta_{002}$, where the subscripts 001 and 002 denote the excess ternary-cluster integrals (the excess over β_3) for the interactions among two middle and one arm-end segments and among two middle and one junction point segments, respectively.

The thick solid and dashed lines in Figure 6, calculated from eqs 9–11 for $f = 4$ with $\beta_3 = 4 \times 10^{-3} \, \mathrm{nm}^6$ and $\beta_{3,1} = 0.032 \, \mathrm{nm}^6$ for 4SPS-Bz and $0.016 \, \mathrm{nm}^6$ for 4SPS-Bu, respectively, closely fit the respective data sets. These $\beta_{3,1}$ values happen to be close to those for linear polystyrenes with the corresponding chain ends, *i.e.*, $0.037 \, \mathrm{nm}^6$ for benzyl-PS[30] and $0.012 \, \mathrm{nm}^6$ for butyl-PS[1]; for linear chains ($f = 1$), $\beta_{3,1}$ is defined by[30] $2\beta_{3,1} = \beta_{001} + \beta'_{001}$, with β_{001} or β'_{001} being the excess ternary-cluster integral concerning two middle segments and one of the chain-end segments; note that $\beta_{001} = \beta'_{001}$ for benzyl-PS. The thin solid and dashed lines in the figure show the theoretical values calculated for benzyl-PS and butyl-PS, respectively, with the above $\beta_{3,1}$ values. As noted previously,[1] the larger $\beta_{3,1}$ for benzyl-PS (with a negligibly small β_{01}) than for butyl-PS (with a positive β'_{01}) is in line with the third virial coefficient B_3 for monatomic gas molecules, in that B_3 at or slightly below the Boyle point (where the second virial coefficient B_2 for the gas molecules is zero or negative) can be larger than those in a certain temperature range above the Boyle point (where $B_2 < 0$). The estimated $\beta_{3,1}$ values for 4SPS-Bz and 4SPS-Bu along with the binary-cluster integrals associated with middle and arm-end segments show the same consistency to hold for the two star polymers.

CONCLUSIONS

The present light scattering measurements on low molar mass samples ($3 \times 10^3 < M_w < 1.5 \times 10^4$) of four-arm star polystyrenes with butyl arm ends (4SPS-Bu) and benzyl arm ends (4SPS-Bz) in cyclohexane at 34.5 °C (Θ) show that A_2 for the former is positive and increases with lowering M_w while that for the latter is negative and decreases. The negative A_2

(for 4SPS-Bz) is explained as due to the effects of three-segment interactions and binary interactions between middle and junction point segments. On the other hand, the positive A_2 results from the effect of the butyl arm ends, so that the lowering of the apparent theta temperature with a decrease in M_w discussed in the literature is due to the effect not of three-segment interactions but of the arm ends, at least, for four-arm star polystyrene with butyl ends. The end effect on A_3 is also significant for the two star polystyrenes and stronger for 4SPS-Bz, as was previously found for linear polystyrenes.

REFERENCES

1. T. Mizuno, K. Terao, Y. Nakamura, and T. Norisuye, *Macromolecules*, **38**, 4432 (2005).
2. K. Huber and W. H. Stockmayer, *Macromolecules*, **20**, 1400 (1987).
3. Y. Einaga, F. Abe, and H. Yamakawa, *Macromolecules*, **26**, 6243 (1993).
4. H. Yamakawa, *Macromolecules*, **25**, 1912 (1992).
5. J.-C. Meunier and R. Van Leemput, *Makromol. Chem.*, **147**, 191 (1971).
6. G. C. Berry, *J. Polym. Sci., A-2*, **9**, 687 (1971).
7. J.-G. Zilliox, *Makromol. Chem.*, **156**, 121 (1972).
8. F. Candau, C. Strazielle, and H. Benoit, *Makromol. Chem.*, **170**, 165 (1973).
9. J. E. L. Roovers and S. Bywater, *Macromolecules*, **7**, 443 (1974).
10. N. Khasat, R. W. Pennisi, N. Hadjichristidis, and L. J. Fetters, *Macromolecules*, **21**, 1100 (1988).
11. B. J. Bauer, L. J. Fetters, W. W. Graessley, N. Hadjichristidis, and G. F. Quack, *Macromolecules*, **22**, 2337 (1989).
12. F. Candau, P. Rempp, and H. Benoit, *Macromolecules*, **5**, 627 (1972).
13. B. J. Bauer, N. Hadjichristidis, L. J. Fetters, and J. E. L. Roovers, *J. Am. Chem. Soc.*, **102**, 2410 (1980).
14. B. J. Cherayil, J. F. Douglas, and K. F. Freed, *J. Chem. Phys.*, **87**, 3089 (1987).
15. M. Okumoto, K. Terao, Y. Nakamura, T. Norisuye, and A. Teramoto, *Macromolecules*, **30**, 7493 (1997).
16. T. Altares, D. P. Wyman, V. R. Allen, and K. Meyersen, *J. Polym. Sci., Part A: Polym. Chem.*, **3**, 4131 (1965).
17. D. J. Worsfold, J.-G. Zilliox, and P. Rempp, *Can. J. Chem.*, **47**, 3379 (1969).
18. J.-C. Meunier and R. Van Leemput, *Makromol. Chem.*, **142**, 1 (1971).
19. J. E. L. Roovers and S. Bywater, *Macromolecules*, **5**, 384 (1972).
20. R. W. Pennisi and L. J. Fetters, *Macromolecules*, **21**, 1094 (1988).
21. G. Deželić and J. Vavra, *Croat. Chem. Acta*, **38**, 35 (1966).
22. Y. Einaga, F. Abe, and H. Yamakawa, *J. Phys. Chem.*, **96**, 3948 (1992).
23. G. C. Berry, *J. Chem. Phys.*, **44**, 4550 (1966).
24. C. E. H. Bawn, F. J. Freeman, and A. R. Kamaliddin, *Trans. Faraday Soc.*, **46**, 862 (1950).
25. T. Sato, T. Norisuye, and H. Fujita, *J. Polym. Sci., Part B: Polym. Phys.*, **25**, 1 (1987).
26. Y. Miyaki, Y. Einaga, and H. Fujita, *Macromolecules*, **11**, 1180 (1978).
27. Y. Nakamura, T. Norisuye, and A. Teramoto, *Macromolecules*, **24**, 4904 (1991).
28. H. Yamakawa and T. Yoshizaki, *J. Chem. Phys.*, **119**, 1257 (2003).
29. B. H. Zimm, *J. Chem. Phys.*, **14**, 164 (1946).
30. H. Yamakawa, F. Abe, and Y. Einaga, *Macromolecules*, **27**, 3272 (1994).